

## Hydrogen Abstraction Reaction of Hydroxyl Radical with 1,1-Dibromoethane and 1,2-Dibromoethane Studied by Using Semi-Classical Transition State Theory

V. Saheb<sup>a,\*</sup> and M. Solimannejad<sup>b,\*</sup>

<sup>a</sup>Department of Chemistry, Shahid-Bahonar University of Kerman, Kerman 76169, Iran

<sup>b</sup>Quantum Chemistry Group, Department of Chemistry, Faculty of Sciences, Arak University, Arak 38156-8-8349, Iran

(Received 3 November 2013, Accepted 22 January 2014)

The hydrogen abstraction reaction by OH radical from CH<sub>2</sub>BrCH<sub>2</sub>Br (R1) and CH<sub>3</sub>CHBr<sub>2</sub> (R2) is investigated theoretically by semi-classical transition state theory. The stationary points for both reactions are located by using ωB97X-D and KMLYP density functional methods along with cc-pVTZ basis. Single-point energy calculations are performed at the QCISD(T) and CCSD(T) levels of theory with different basis sets. The results show that the activation energies are very sensitive to the effects of electron correlation and basis set. In order to correct basis set effects on the calculated energetic, a correction factor (CF) is determined from the energy difference between the MP2/cc-pVTZ and MP2/aug-cc-pVTZ levels.  $x_{ij}$  vibrational anharmonicity coefficients, needed for semi-classical transition state theory, are calculated at the KMLYP/cc-pVTZ level of theory. Thermal rate coefficients are computed over the temperature range from 200 to 3000 K and they are shown to be in accordance with available experimental data. The computed rate constants for the reactions R1 and R2 are fitted to the equation

$$k(T) = AT^n \exp[-E(T + T_0)/(T^2 + T_0^2)]$$

**Keywords:** Dibromoethane, Hydroxyl radical, *Ab initio*, Semi-classical transition state, Rate constants

### INTRODUCTION

The reactions of hydroxyl radicals with various halogenated hydrocarbons have received considerable studies because of their importance in atmospheric and combustion processes [1]. Halogen-containing gases, recognized as ozone-depleting chemicals, are emitted at the Earth's surface and accumulated in the troposphere and transported to the stratosphere [2]. The OH radicals, known as atmospheric detergents, are the main oxidizer in the tropospheric degradation of halocarbons containing H atoms.

Bromine-containing gases in the atmosphere are of

anthropogenic and natural origin. In the ocean, marine organisms are estimated to produce 1-2 billion kilograms of CH<sub>3</sub>Br annually [3]. Of the nearly 3200 known naturally occurring organohalogen compounds, more than 1600 contain bromine [3]. Many organobromine compounds have been used as fire-retardants, fumigants and biocides, dyes and pharmaceuticals. For sometime 1,2-dibromoethane was of commercial significance as a component of leaded gasoline and a popular fumigant in agriculture. As a consequence, many laboratories have studied the reactions of OH radicals with 1,2-dibromoethane and 1,1-dibromoethane [4-10].



\*Corresponding authors. E-mail: vahidsaheb@mail.uk.ac.ir; m-solimannejad@araku.ac.ir



In a pioneering study, Howard and Evenson [4] used a discharge-flow system equipped with a laser magnetic resonance device for detection of OH and obtained a value of  $1.58 \times 10^8 \text{ l mol}^{-1} \text{ s}^{-1}$  for the absolute rate constant of the reaction R1 at 296 K. Arnsts and coworkers [5] studied the reaction R1 in a low flow system along with gas chromatograph for analysis of the products and obtained a value of  $1.45 \times 10^8 \text{ l mol}^{-1} \text{ s}^{-1}$  at 296 K. The discharge flow-resonance fluorescence method was used by Qiu *et al.* [7] to measure the rate constants of OH reactions with 1,2-dibromoethane and the Arrhenius expression  $k_1 = 8.79 \times 10^9 \text{ l mol}^{-1} \text{ s}^{-1} \exp(-10.65 \text{ kJ mol}^{-1}/\text{RT})$  was obtained over the temperature range from 292 to 366 K. In the latest study, Xing *et al.* [8] measured the rate constants of the reactions R1 and R2 by using a discharge flow-resonance fluorescence technique and obtained the Arrhenius expression  $k_1 = 8.65 \times 10^9 \text{ l mol}^{-1} \text{ s}^{-1} \exp(-10.54 \text{ kJ mol}^{-1}/\text{RT})$  for the reaction R1 over the temperature range from 293 to 418 K. To the best of our knowledge, the later study is the only experimental investigation performed on the kinetics of the reaction between OH radical and 1,1-dibromoethane in which the overall rate constant (the sum of the reaction channels R2A and R2B) is measured and the Arrhenius expression  $k_2 = 1.41 \times 10^{10} \text{ l mol}^{-1} \text{ s}^{-1} \exp(-10.70 \text{ kJ mol}^{-1}/\text{RT})$  is reported. In 1987, Cohen and Benson have estimated the barrier height of the reaction R1 by bond energy-bond order (BEBO) method [10]. They have used approximate methods to evaluate molecular parameters of the reactants and transition state and calculated the thermal rate coefficients by conventional transition state theory.

In this research, we have attempted to employ high-level quantum chemical methods to investigate the potential energy surfaces of the title reactions. Then, Semi-Classical Transition State Theory (SCTST) is used to compute the rate constants of the reactions.

## Computational Details

**Electronic-structure calculations.** In the present study, the commonly used Beck's three-parameter exchange functional [11] with Lee, Yang and Parr's [12] correlation functional (B3LYP) is used to optimize the geometries of all of the stationary points, *i.e.*, minimum energy structures and

saddle points. The KMLYP method which is a mix of Slater exchange and exact exchange for the exchange functional and a mix of the correlation functional of Vosko, Wilk, Nusair (VWN) and that of Lee, Yang, and Parr (LYP) [13], is also used to re-optimize the geometries, energies and ro-vibrational properties of all of the stationary points. The later hybrid density-functional method is optimized against 132 data, including 74 transition state barriers and 58 enthalpies of reaction and it is shown that it predicts transition state barriers with the same accuracy as CBS-APNO, and transition state barriers and enthalpies of reaction with smaller errors in comparison with B3LYP, BHandHLYP, and G2. The long-range corrected hybrid density functional proposed by Chai and Head-Gordon [14],  $\omega\text{B97X-D}$ , is also used. This functional has yielded satisfactory accuracy for thermochemistry, kinetics, and non-covalent interactions.

In order to compute accurate energies, single-point energy calculations are performed with the unrestricted coupled cluster method with single, double, and noniterative triple excitations uCCSD(T) [15] and the unrestricted quadratic configuration interaction with single, double, and noniterative triple excitations uQCISD(T) [16] in combination with the correlation-consistent polarized triple- $\zeta$  basis set cc-pVTZ [17] and the standard 6-311+G(3df,2p) basis sets. Single-point energy calculations at the CCSD(T) level of theory using a larger basis set (*e.g.*, aug-cc-pVTZ) are extremely computationally demanding. We have corrected basis set effects on the calculated energies by the same procedure developed and employed by Zhang and coworkers for systems with too many electrons [18,19]. In this procedure, a correction factor associated with basis set effects at the MP2 level is determined. Subsequently, the correction factor is added to the energy calculated at a higher level of electron correlation with a moderate size basis set. In the present research, a correction factor (CF) is determined from the energy difference between the MP2/cc-pVTZ and MP2/aug-cc-pVTZ levels. The values of calculated energies at the CCSD(T)/cc-pVTZ level are then corrected by the MP2 level correction factors, corresponding to the CCSD(T)/cc-pVTZ + CF method.

Harmonic vibrational frequencies and  $x_{ij}$  vibrational anharmonicity coefficients are calculated at the KMLYP/cc-pVTZ level of theory. All of the quantum chemical

calculations are performed with the Gaussian09 package of programs [20].

**Semi-classical transition state theory.** SCTST was developed by Miller and colleagues [21-24]. According to the SCTST, canonical rate constant is given by following equation:

$$k(T) = \frac{1}{h} \frac{\int_0^{\infty} G^{\ddagger}(E) \exp(-E/k_B T) dE}{Q_{re}(T)} \quad (1)$$

where  $h$  is Planck's constant,  $k_B$  is Boltzmann's constant,  $T$  is the temperature,  $Q_{re}$  is the total partition function of the reactant(s), and  $G^{\ddagger}(E)$  is the cumulative reaction probability (CRP). At moderate temperatures, couplings between rotations and vibrations can be neglected, giving

$$k(T) = \frac{1}{h} \frac{Q_t^{\ddagger} Q_r^{\ddagger} \int_0^{\infty} G_v^{\ddagger}(E_v) \exp(-E_v/k_B T) dE_v}{Q_t Q_r Q_v(T)} \quad (2)$$

where the  $Q_t$ ,  $Q_r$  and  $Q_v$  represent the translational, rotational and vibrational partition functions for the reactants, respectively, and the  $Q_t^{\ddagger}$ ,  $Q_r^{\ddagger}$  and  $Q_v^{\ddagger}$  represent corresponding values for transition state. Vibrational energy of transition state,  $E_v$ , is the variable of integration. The cumulative reaction probability is given by

$$G_v^{\ddagger}(E_v) = \sum_{n_1} \sum_{n_2} \dots \sum_{n_{F-2}} \sum_{n_{F-1}} P_n(E_v) \quad (3)$$

where the semiclassical tunneling probability  $P_n$  is obtained from the following expression:

$$P_n(E) = \frac{1}{1 + \exp[2\theta(n, E)]} \quad (4)$$

The barrier penetration integral  $\theta(n, T)$  is given by

$$\theta(n, E) = \frac{\pi \Delta E}{\Omega_F} \frac{2}{1 + \sqrt{1 + 4x_{FF} \Delta E / \Omega_F^2}} \quad (5)$$

where  $\Delta E$  and  $\Omega_F$  are computed from the following

expressions:

$$\Delta E = \Delta V_0 + \varepsilon_0 - E + \sum_{k=1}^{F-1} \omega_k \left( n_k + \frac{1}{2} \right) + \sum_{k=1}^{F-1} \sum_{l=k}^{F-1} x_{kl} \left( n_k + \frac{1}{2} \right) \left( n_l + \frac{1}{2} \right) \quad (6)$$

$$\Omega_F = \bar{\omega}_F - \sum_{k=1}^{F-1} \bar{x}_{kF} \left( n_k + \frac{1}{2} \right) \quad (7)$$

$$\bar{\omega}_F = -i\omega_F \quad \text{and} \quad \bar{x}_{kF} = -ix_{kF} \quad (8)$$

In the above expressions,  $F$  is the number of internal degrees of freedom of the transition state, ordered so that the reaction coordinate is last,  $\omega_k$  is the harmonic vibrational frequency of the  $k_{th}$  vibration,  $\omega_F$  is the imaginary frequency associated with the reaction coordinate,  $x_{kl}$  are the vibrational anharmonicity constants for the degrees of freedom orthogonal to the reaction coordinate,  $x_{kF}$  are the (pure imaginary) coupling terms between the reaction coordinate and the orthogonal degrees of freedom,  $x_{FF}$  is the (pure real) anharmonicity constant for the reaction path, and  $\Delta V_0$  is the classical barrier height. The term  $\varepsilon_0$  is a constant which is included for thermochemistry and kinetics. The SCTST is a powerful method because all of the degrees of freedom including reaction coordinate are assumed to be coupled. It also accounts naturally for zero point energy and quantum mechanical tunneling along the curved reaction path in hyperdimensional space.

In Eqs. (1) and (2), the CRP is obtained by summing over all states of the transition state. In this research, the Nguyen-Barker algorithm [25-27] is used for computing the partition functions and CRP for the fully coupled anharmonic vibrations of reactants and transition states, respectively. The Nguyen-Barker algorithm is based on the Wang and Landau [28,29] random walk algorithm in energy space for computing densities of states for the use in classical statistical models. On the basis of the Wang-Landau algorithm, Basire *et al.* [30] have used the perturbation theory expansion for vibrational energy of fully coupled anharmonic systems to compute quantum densities of states. Nguyen and Barker have modified the Basire *et al.*

algorithm in several minor ways to meet the needs for the density of states and cumulative reaction probabilities in chemical kinetics. Computer programs SCTST and ADENSUM, developed by Barker and colleagues, are used for computing the CRPs of transition states and the partition functions of the reactants, respectively. The program THERMO is used to compute the thermal rate constants; all three codes are included in the MULTIWELL Program Suite [31].

All low-frequency torsional vibrational motions are considered as hindered internal rotations. The torsional potential energies are computed at the KMLYP/cc-pVTZ and fitted to the following general equation:

$$V(\chi) = V_0 + \sum_{n=1}^N V_n^c \cos(n\sigma_v(\chi + \varphi_v)) + \sum_{n=1}^N V_n^s \sin(n\sigma_v(\chi + \varphi_v)) \quad (9)$$

The ro-vibrational G matrix-based algorithm described by Harthcock and Laane [32,33] is used to compute the effective reduced mass for one-dimensional torsions as functions of the dihedral angle  $\chi$  (radians) and fitted to the following general equation:

$$I(\chi) = I_0 + \sum_{n=1}^N I_n \cos(n\sigma_I(\chi + \varphi_I)) \quad (10)$$

Computer programs lamm [31], developed by Nguyen and contained in the MULTIWELL Program Suite, is used to compute the effective reduced masses. The Fourier coefficients in the Eqs. (9) and (10) are used by programs ADENSUM to solve the Schrödinger equation for the energy eigenstates, which are needed to compute densities of states.

## RESULTS AND DISCUSSION

The reactions R1, R2A and R2B proceed through transition state structures TS1, TS2A and TS2B leading to  $\text{CHBrCH}_2\text{Br}^\cdot + \text{H}_2\text{O}$ ,  $\text{CH}_2\text{CHBr}_2^\cdot + \text{H}_2\text{O}$  and  $\text{CH}_3\text{CBr}_2^\cdot + \text{H}_2\text{O}$ , respectively. The geometries of reactants and transition states of the title reactions optimized at two levels of theory are shown in Fig. 1. The relative energies of the stationary points located on the potential energy surface of

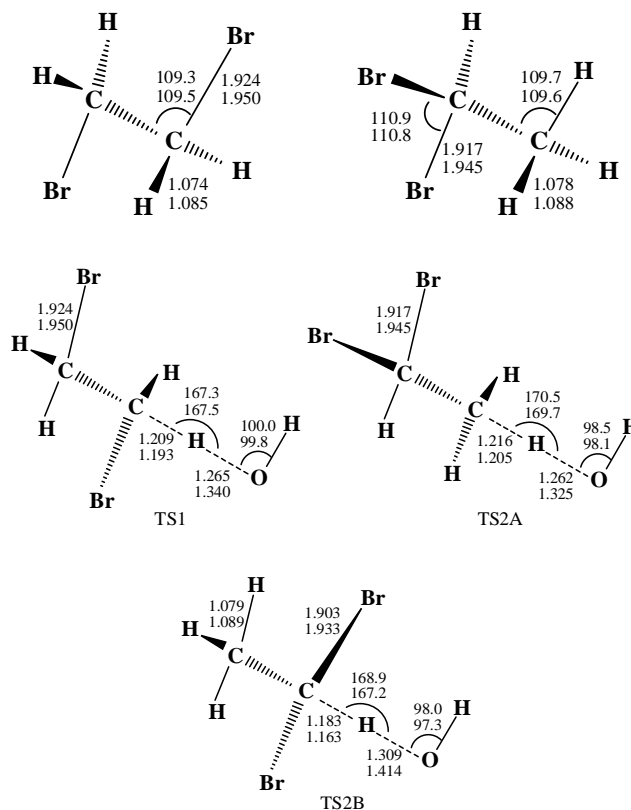


**Fig. 1.** The geometries of reactants and transition states of the reactions R1, R2A and R2B, respectively. The top and bottom values are calculated at the KMLYP/cc-pVTZ and  $\omega$ B97X-D/cc-pVTZ, respectively.

the reactions R1, R2A and R2B computed at various levels of theory are listed in Table 1. As can be seen from Fig. 1 and Table 1, consistent geometries and energies are obtained for stationary points of this reaction at various levels of theory. The harmonic vibrational frequencies and the principle moments of inertia of the reactants and transition states, calculated at the KMLYP/cc-pVTZ level of theory, are provided in Table 1S in the Supplementary Information. Tables 2S, 3S and 4S provide the anharmonicity constants matrices for the transition states of the reactions R1, R2A and R2B, respectively. As mentioned in the theoretical section, the low vibrational frequencies (underlined in Table 1S), corresponding to torsional vibrational motions, are treated as hindered internal rotations. First, molecular geometries and energies are

**Table 1.** The Relative Energies of the Stationary Points for Reaction R1, R2A, and R2B Computed at Various Levels of Theory in  $\text{kJ mol}^{-1}$ . All Values are Corrected for Zero Point Energies<sup>†</sup>

	TS1	TS2A	TS2B	$\text{CHBrCH}_2\text{Br}+\text{H}_2\text{O}$	$\text{CH}_2\text{CHBr}_2+\text{H}_2\text{O}$	$\text{CH}_3\text{CBr}_2+\text{H}_2\text{O}$
$\omega\text{B97X-D}$	-6.44	-3.09	-11.14	-97.37	-69.30	-95.27
KMLYP	12.69	12.90	5.24	-76.09	-63.73	-92.24
QCISD(T)	5.40 (7.17)	8.88 (9.60)	-0.29 (-1.30)	-78.11 (-82.38)	-64.17 (-69.56)	-89.65 (-95.66)
CCSD(T)	6.48 (8.36)	10.03 (10.58)	1.13 (0.00)	-77.43 (-81.64)	-63.57 (-69.16)	-88.73 (-94.96)
CCSD(T)+CF	2.28	6.54	-2.08	-80.35	-68.31	-91.82

<sup>†</sup>The standard basis set 6-311+G(3df,2p) are used for the values in the parentheses. The cc-pVTZ basis set is used along with other values.

computed at discrete values of torsional angles,  $\chi$ , at the KMLYP/cc-pVTZ level of theory. Then, the effective reduced masses for one-dimensional torsions are computed by using the ro-vibrational G matrix-based algorithm of Harthcock *et al.* [32,33]. The computed potential energies and reduced moments of inertia are fitted to the Eqs. (9) and (10), respectively. The fitted values of parameters for torsional motions of the reactants and transition states are provided in the Supplementary Information.

On the basis of the information obtained from Tables 1 and 1S to 5S, SCTST is used to calculate the thermal rate coefficients of the reactions R1, R2A and R2B over the temperature range of 200 to 3000 K. Figure 2 shows the computed rate coefficients for the reaction R1 in comparison with the literature data. In order to investigate the significance of low-frequency vibrations in computed rate constants, two additional calculations are also undertaken. In the first calculations, two low-frequency vibrations of transition states are considered as coupled vibrational frequencies (line 3 in the Fig. 2). In the second calculations, two low-frequency vibrations are neglected in the calculation of partition functions (line 4 in the Fig. 3). Although the values computed by the former model are relatively close to the previous calculations at low

temperatures, inconsistent results are obtained at high temperatures. As mentioned in Introduction, Cohen and Benson [10] have investigated the reaction R1 by approximate methods. They found that calculations for both free and slightly hindered internal rotations are in better agreement with experimental data. Their computed rate constants are depicted in Fig. 2 for the purpose of comparison.

When the low frequencies are neglected in the calculations, the computed rate coefficients decrease from 3 times at 200 K to 1000 times at 3000 K. It is found that tunneling has a negligible effect on the computed rate constants due to the very low barrier heights. The calculated rate constants are found to be sensitive to the computed barrier heights. As can be seen from Fig. 2, the rate coefficients computed by using CCSD(T)/cc-pVTZ + CF barrier heights (line 2) are in accordance with the experimental data. The values are slightly underestimated by using CCSD(T)/cc-pVTZ barrier height (line 1).

As mentioned in Introduction, there is only one experimental study on the kinetics of the reaction between OH radical and 1,1-dibromoethane in which the overall rate constant (the sum of the reaction channels R2A and R2B) is measured. The computed overall rate constants for the

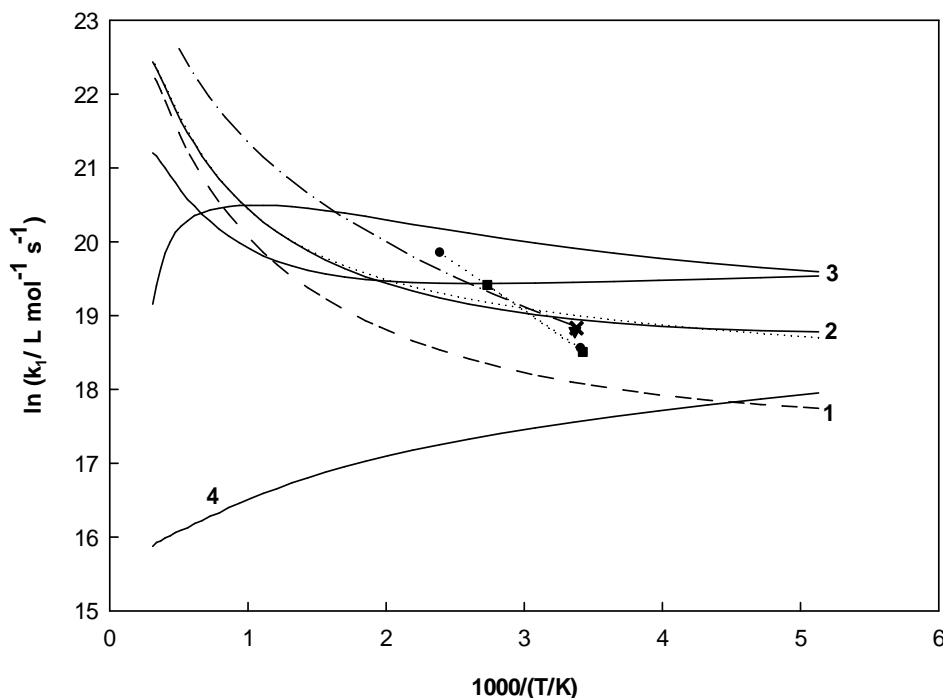


**Fig. 2.** The thermal rate coefficients for the reaction channel R1 computed at temperatures in the range of 200-3000 K. “Line 1” is calculated using CCSD(T)/cc-pVTZ barrier height, “line 2” using CCSD(T)/cc-pVTZ+CF barrier height, “line 3” using CCSD(T)/cc-pVTZ+CF barrier height while low-frequency vibrations are not considered as hindered rotations, “line 4” using CCSD(T)/cc-pVTZ+CF barrier height while low-frequency vibrations are neglected, “dash-dotted line” is calculated by Cohen and Benson (Ref. 10). Experimental data for the channel R1 are given for the purpose of comparison. (x) from Ref. 4, (▼) from Ref. 5, (■) from Ref. 7, (●) from Ref. 10.

reaction R2 are shown in Fig. 3 in comparison with the latter experimental data. The significance of the low-frequency vibrations is also studied for this reaction. Essentially the same conclusions as the reaction R1 are drawn for the reaction R2. The three-parameter Arrhenius equation which is widely used for representing the temperature-dependence of the rate coefficients is  $k(T) = AT^n e^{-E/RT}$ , where A, n, and E are parameters and T is temperature. It is found that the latter equation cannot fit perfectly the curved Arrhenius plots in wide temperature ranges, especially at low temperatures. Zheng and Truhlar [34] have shown that the following elaborate expression reproduces the rate constants over wide temperature ranges:

$$k(T) = AT^n \exp\left[\frac{-E(T+T_0)}{T^2+T_0^2}\right] \quad (11)$$

As the main product of the present study, the computed rate constants for reactions R1 and R2 by using CCSD(T)/cc-pVTZ + CF barrier heights are fitted to the equation 11. The fitted parameters A, n, E, and  $T_0$  are given in Table 2. The suggested rate expressions for the reaction R1 is compared with the computed rate constants in the Supplementary Information. The experimental activation energy is defined as  $E_a = -Rd(\ln k)/d(1/T)$ . It is concluded from Figs. 2 and 3 that activation energies of the reaction R1 and R2 are very low (close to zero) at temperatures below 1000 K. However,

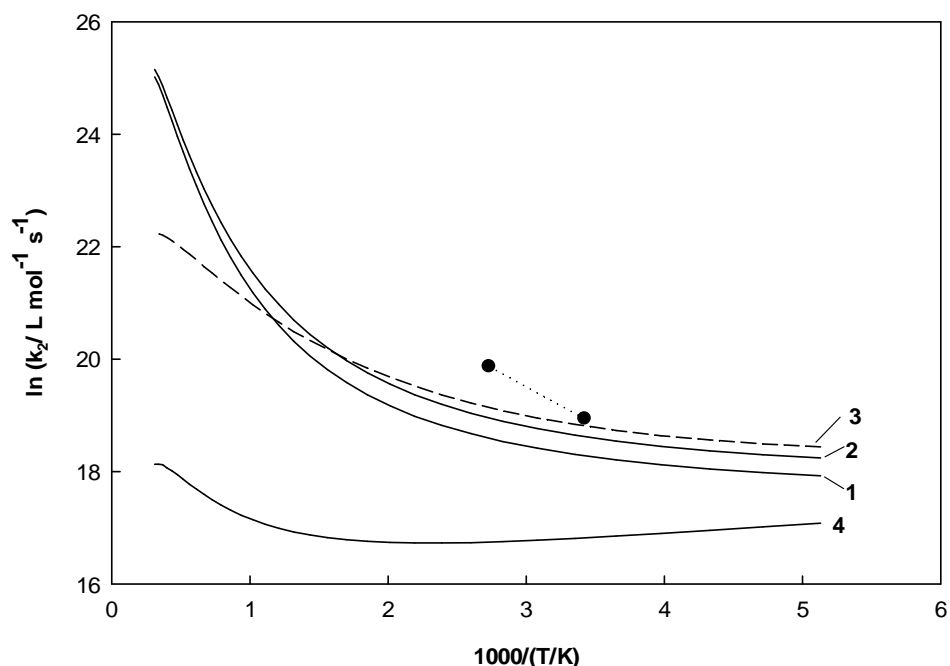


**Fig. 3.** The thermal rate coefficients for the reaction channel R2 computed at temperatures in the range of 200-3000 K. “Line 1” is calculated using CCSD(T)/cc-pVTZ barrier height, “line 2” using CCSD(T)/cc-pVTZ+CF barrier height, “line 3” using CCSD(T)/cc-pVTZ+CF barrier height while low-frequency vibrations are not considered as hindered rotations, “line 4” using CCSD(T)/cc-pVTZ+CF barrier height while low-frequency vibrations are neglected. (●) from Ref. 7.

**Table 2.** Fitted Parameters of Zheng and Truhlar’s Rate Constant Expression for the Reactions R1 and R2 (the Sum of R2A and R2B).

Parameters	Reaction R1	Reaction R2
A	$1.395 \times 10^8$	$2.29 \times 10^{11}$
n	0.42	-0.2033
E	-5859	-16049.8
T <sub>0</sub>	-2358	-2154.3

activation energies increase at higher temperatures.

## CONCLUSIONS

In this research, electronic structure theories are employed to compute the energies and other molecular

properties of the stationary points on the potential energy surfaces of the H-abstraction reaction of hydroxyl radical with 1,2-dibromoethane and 1,1-dibromoethane. All geometries are optimized by  $\omega$ B97X-D and KMLYP methods along with cc-pVTZ. Single-point energy calculations are performed at the QCISD(T) and CCSD(T)

levels of theory on the optimized geometries by KMLYP method. A correction factor (CF) is determined from the energy difference between the MP2/cc-pVTZ and MP2/aug-cc-pVTZ levels. The vibrational frequencies and vibrational anharmonicity constants are computed at the KMLYP/cc-pVTZ level. Semi-classical transition state theory is employed to calculate the thermal rate coefficients. The calculated rate constants, by employing the barrier heights computed at the CCSD(T)/cc-pVTZ + CF level, are in accordance with the available experimental data.

## REFERENCES

- [1] R. Atkinson, *Chem. Rev.* 86 (1986) 69.
- [2] M.P. Chipperfield, W.J. Randel, G.E. Bodeker, *et al.*, *Global Ozone: Past and Future*, Chapter 4, *Global Ozone Research and Monitoring Project-Report No. 47* (2003) 498.
- [3] G.W. Gribble, *Chem. Soc. Rev.* 28 (1999) 335.
- [4] C.J. Howard, K.M. Evenson, *J. Chem. Phys.* 64 (1976) 4303.
- [5] R.R. Arnts, R.L. Seila, J.J. Bufalini, *J. Air Pollut. Control Assoc.* 39 (1989) 453.
- [6] N. Cohen, K.R. Westberg, *J. Phys. Chem. Ref. Data* 20 (1991)1211.
- [7] L.X. Qiu, S.H. Shi, S.B. Xing, X.G. Chen, *J. Phys. Chem.* 96 (1992) 685.
- [8] S.B. Xing, S.H. Shi, L.X. Qiu, *Int. J. Chem. Kinet.* 24 (1992) 1.
- [9] C. Chiorboli, R. Piazza, M.L. Tosato, V. Carassiti, *Coord. Chem. Rev.* 125 (1993) 241.
- [10] N. Cohen, S.W. Benson, *J. Phys. Chem.* 91 (1987)162.
- [11] A.D. Becke, *J. Chem. Phys.* 98 (1993) 5648.
- [12] C. Lee, W. Yang, R.G. Parr, *Phys. Rev. B* 37 (1988) 785.
- [13] J.K. Kang, C.B. Musgrave, *J. Chem. Phys.* 115 (2001) 11040.
- [14] J.D. Chai, M. Head-Gordon, *Phys. Chem. Chem. Phys.* 10 (2008) 6615.
- [15] K. Raghavachari, G.W. Trucks, J.A. Pople, M. Head-Gordon, *Chem. Phys. Lett.* 157 (1989) 479.
- [16] J.A. Pople, M. Head-Gordon, K. Raghavachari, *J. Chem. Phys.* 87 (1987) 5968.
- [17] R.A. Kendall, T.H. Dunning, R.J. Harrison, *J. Chem. Phys.* 96 (1992) 6796.
- [18] W. Lei, A. Derecskei-Kovacs, R. Zhang, *J. Chem. Phys.* 113 (2000) 5354.
- [19] D. Zhang, R. Zhang, *J. Am. Chem. Soc.* 124 (2002) 2692.
- [20] M.J. Frisch, G.W. Trucks, H.B. Schlegel, *et al.*, GAUSSIAN 09, Gaussian, Inc., Wallingford, CT, 2009.
- [21] W.H. Miller, *J. Chem. Phys.* 62 (1975) 1899.
- [22] W.H. Miller, *Faraday Discuss. Chem. Soc.* 62 (1977) 40.
- [23] W.H. Miller, R. Hernandez, N.C. Handy, D. Jayatilaka, A. Willets, *Chem. Phys. Lett.* 172 (1990) 62.
- [24] R. Hernandez, W.H. Miller, *Chem. Phys. Lett.* 214 (1993)129.
- [25] T.L. Nguyen, J.R. Barker, *J. Phys. Chem. A.* 114 (2010) 3718.
- [26] T.L. Nguyen, J.F. Stanton, J.R. Barker, *Chem. Phys. Lett.* 499 (2010) 9.
- [27] T.L. Nguyen, J.F. Stanton, J.R. Barker, *J. Phys. Chem. A* 115 (2011) 5118.
- [28] F. Wang, D.P. Landau, *Phys. Rev. Lett.* 86 (2001) 2050.
- [29] F. Wang, D.P. Landau, *Phys. Rev. E* 64 (2001) 56101.
- [30] M. Basire, P. Parneix, F. Calvo, *J. Chem. Phys.* 129 (2008) 081101.
- [31] J.R. Barker, N.F. Ortiz, J.M. Preses, L.L. Lohr, A. Maranzana, P.J. Stimac, T.L. Nguyen, T.J.D. Kumar, *MultiWell-2010.2 Software*, University of Michigan, Ann Arbor, Michigan, 2010, <http://aoss.engin.umich.edu/multiwell/>.
- [32] M.A. Harthcock, J. Laane, *J. Mol. Spectros.* 91 (1982) 300.
- [33] M.A. Harthcock, J. Laane, *J. Phys. Chem.* 89 (1985) 4231.
- [34] J. Zheng, D.G. Truhlar, *Phys. Chem. Chem. Phys.* 12 (2010) 7782.